www.czasopisma.pan.pl PAN POLSKA AKADEMIA NAUK www.journals.pan.pl

Arch. Metall. Mater. **62** (2017), 4, 1963-1968

DOI: 10.1515/amm-2017-0294

B. ERTUĞ*#, B. NILGÜN ÇETINER***, H. GÖKÇE**, Z. ENGIN ERKMEN***, M. LÜTFI ÖVEÇOĞLU**

INVESTIGATION OF INDENTATION FRACTURE TOUGHNESS (K_{IC}) AND WEIBULL PARAMETERS OF $0.25Li_2O.2SiO_2$-$0.75BaO.2SiO_2$ GLASS-CERAMIC

In the present study, mechanical properties of $0.25Li_2O.2SiO_2$-$0.75BaO.2SiO_2$ glass-ceramic were investigated. The transformations' temperatures were determined by DTA instrument. The optimum nucleation temperature was found to be 540°C. This suggested the crystallization temperatures as 675, 720 and 800°C. After carrying out crystallization heat treatments, Vickers indentation test was applied. In order to determine the indentation fracture toughness (K_{IC}), crack half-length ‚c' of the samples was measured. To calculate K_{IC}, Young's modulus, E and the measured hardness, H_v were used. Using K_{IC} and probability of fracture ‚P', $\ln \ln[1/(1-P)] - \ln K_{IC}$ graph was drawn based on the Weibull distribution equation. Consequently, Weibull modulus, ‚m' and scale parameter, ‚K_0' were determined and compared with each other.

Keywords: Lithium barium silicate glass-ceramic, Indentation Fracture Toughness, Hardness, Statistical Analysis, Weibull modulus.

1. Introduction

Fracture of ceramics in general starts from flaws, which are spread throughout. The higher the load, the larger the probability of the failure. Also, the failure probability changes with the sample size. According to Griffith/Irwin equation, when stress intensity factor $K = s.Y(p.a)^{-1/2}$ exceeds the fracture toughness, K_{IC} one can estimate the formation of critical flaws. This equation shows the relationship between the flaw size and critical load [1]. Weibull modulus (m) is widely used to evaluate the structural reliability of the material. The higher the Weibull modulus, the higher the structural reliability [2]. For technical ceramics, the value of the Weibull modulus is between 5 and 20 [3].

The probability of failure changes with distribution of the weak stress regions. Over these weak stress regions, the crack starts and propagates. These regions are related to the fracture toughness of the material. Thus the Weibull statistics and fracture toughness are closely related [4]. Ceramics in general, possess higher hardnesses than metallic materials. However, they indicate poor toughness and low strength reliability. Low Weibull moduli show highly variable crack length in the material exhibiting broad strength distribution [5]. If the type of the distribution function is known, the number of experiments can be reduced, because only a few parameters and not the distribution function in each detail must be determined. In the case of the Gaussian and Poisson distributions, the parameters are the mean value and the standard deviation. For the Weibull distribution, the parameters are the characteristic strength and the Weibull modulus [6].

In the present paper, it was attempted to characterize a novel glass-ceramic composition. Main properties such as Vickers microhardness and indentation fracture toughness were examined. In addition, structural reliability of the samples was evaluated using Weibull parameters derived from the experimental results.

2. Experimental procedure

The details of the preparation of $0.25Li_2O.2SiO_2$-$0.75BaO.2SiO_2$ glass-ceramic were given elsewhere [7]. Glasses were heat treated initially at 540°C / 3h, secondly at 675, 720 or 800°C for 1 h. After surface finishing, the microstructural evolution of the crystallized samples were examined by Scanning Electron Microscope (SEM) equipped with EDS (Energy Dispersive Spectroscopy) analyzer. In order to determine the phase transformation peaks, Differential Thermal Analysis (DTA) was applied using Netzsch STA 409 CD. Schimadzu Vickers indenter was used to perform indentations during 30 s under 0.2 kg for microhardness and 0.5-1 kg for fracture toughness measurements, respectively. Following the tests, symmetrical indentations and cracks were observed and the crack lengths were measured using optical system attached in Vickers tester.

* NIŞANTAŞI UNIVERSITY, DEPARTMENT OF MECHANICAL ENGINEERING, 34406 KAĞITHANE, ISTANBUL, TURKEY
** ISTANBUL TECHNICAL UNIVERSITY, DEPARTMENT OF METALLURGICAL AND MATERIALS ENGINEERING, 34469 MASLAK, ISTANBUL, TURKEY
*** MARMARA UNIVERSITY, DEPARTMENT OF METALLURGICAL AND MATERIALS ENGINEERING, 34722 GÖZTEPE, ISTANBUL, TURKEY
# Corresponding author: burcu.ertug@nisantasi.edu.tr

3. Results and discussion

The optimum nucleation temperature of $0.25Li_2O.2SiO_2$-$0.75BaO.2SiO_2$ glass was determined by Marotta method [8]. According to this method and DTA, glasses were nucleated above the glass transition temperature, T_g were obtained and compared to that of as-cast glass. In Fig. 1, DTA curves of nucleated glasses at 490-550°C for 1h were shown including the crystallization temperatures. Fig. 2 indicates a typical Marotta curve in which the crystallization temperature change is shown versus nucleation temperature. According to Fig. 1, for the glass nucleated at 540°C for 1h, the crystallization peak corresponds to exothermic reaction at 712°C, which is the lowest among other nucleated glasses. The endothermic reactions seen in the DTA curves, approximately at 980°C, can be related to the melting of this composition following nucleation at different temperatures.

Fig. 3, 4 and 5 show SEM images of the crystallized samples at 675, 720 and 800°C, together with the SEM images and corresponding EDS analysis results were given. All the SEM images show a dual crystallite phases in the microstructures. These phases were observed as white and dark regions using BSE (Back Scattering Electron Analysis). Fig. 3 indicates a low magnification image of the sample crystallized at 675°C for 1 h. A slight radial symmetry can be observed at this magnification. At higher magnification, two distinct phases were present. The same radial crystal growth was also observed by Zheng et al. when crystallization temperature was around 600°C, which is similar to the present study [9]. EDS analysis performed at points 1 and 2 indicated low and high Ba element content, respectively showing

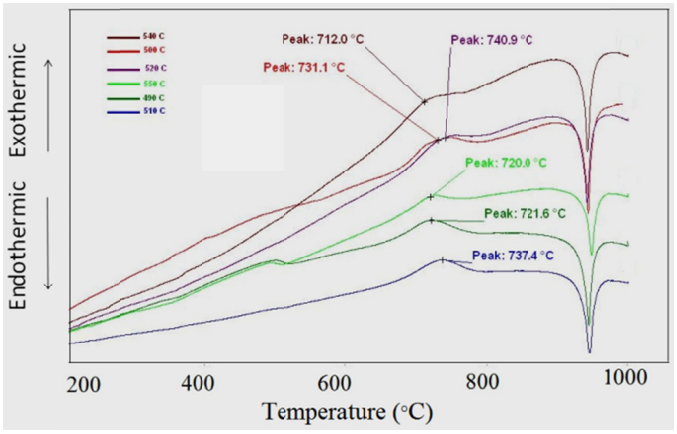

Fig. 1. DTA analysis of nucleated glasses for $0.25Li_2O.2SiO_2$-$0.75BaO.2SiO_2$

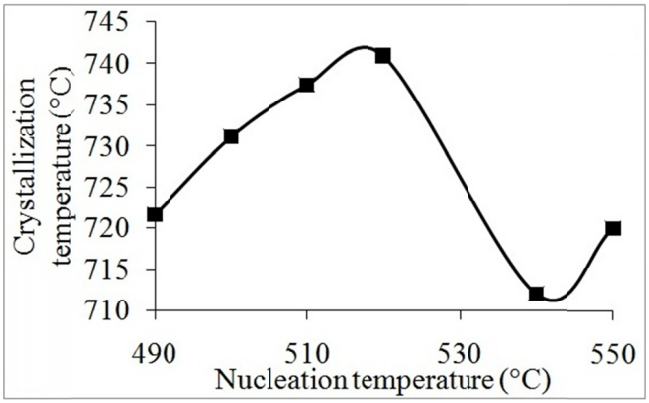

Fig. 2. Marotta curve for $0.25Li_2O.2SiO_2$-$0.75BaO.2SiO_2$

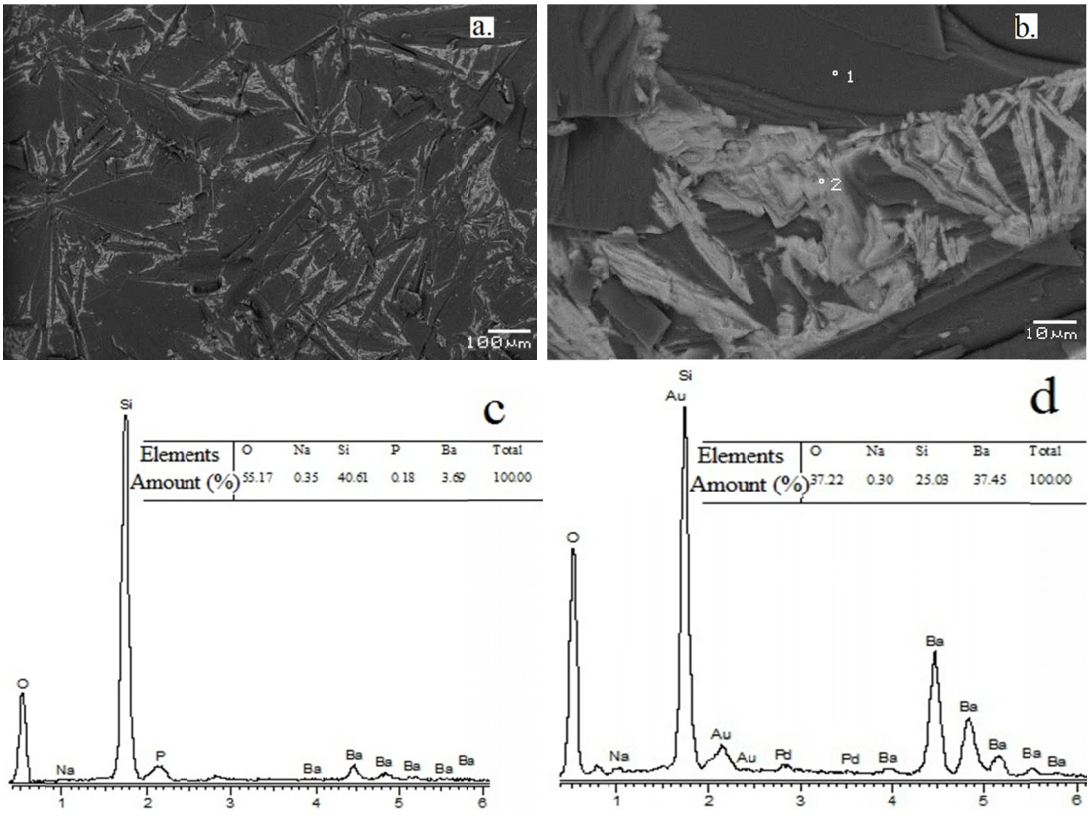

Fig. 3. (a-b) SEM images and (c-d) EDS analysis of the samples heat treated at) 675°C

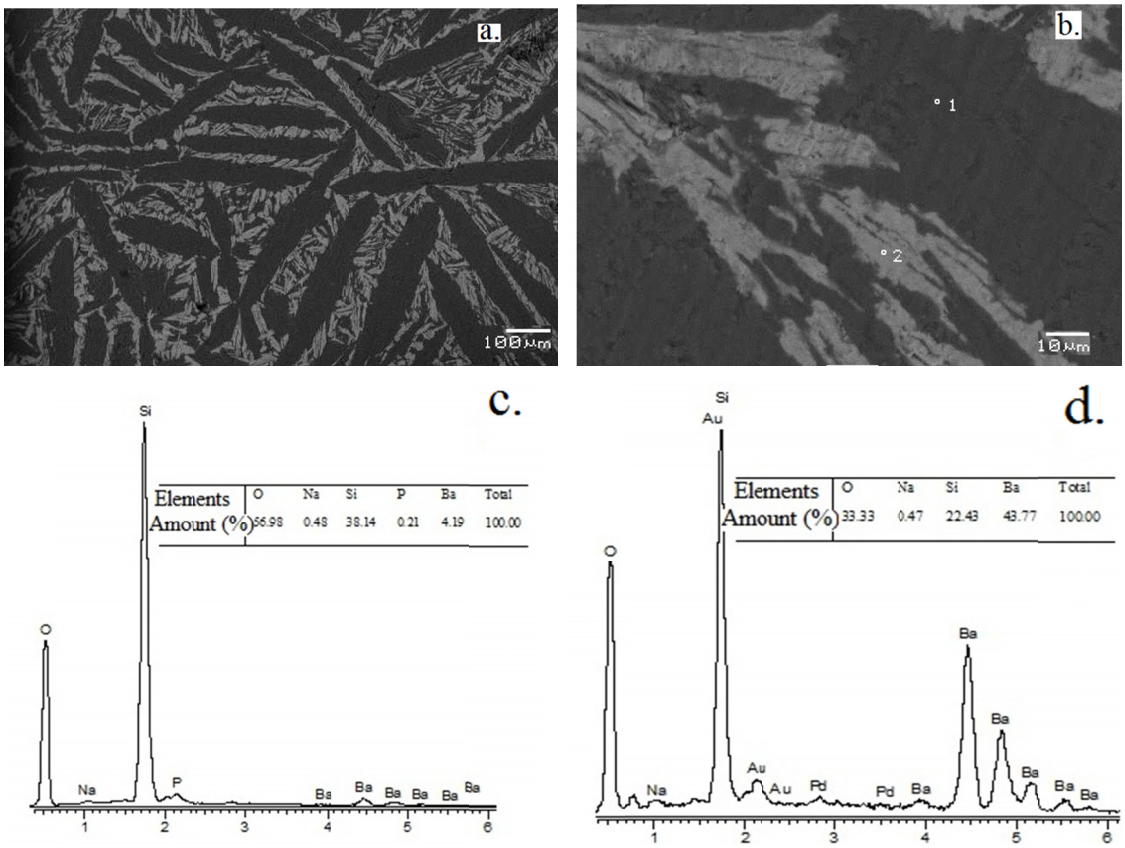

Fig. 4. (a-b) SEM images and (c-d) EDS analysis of the samples heat treated at 720°C

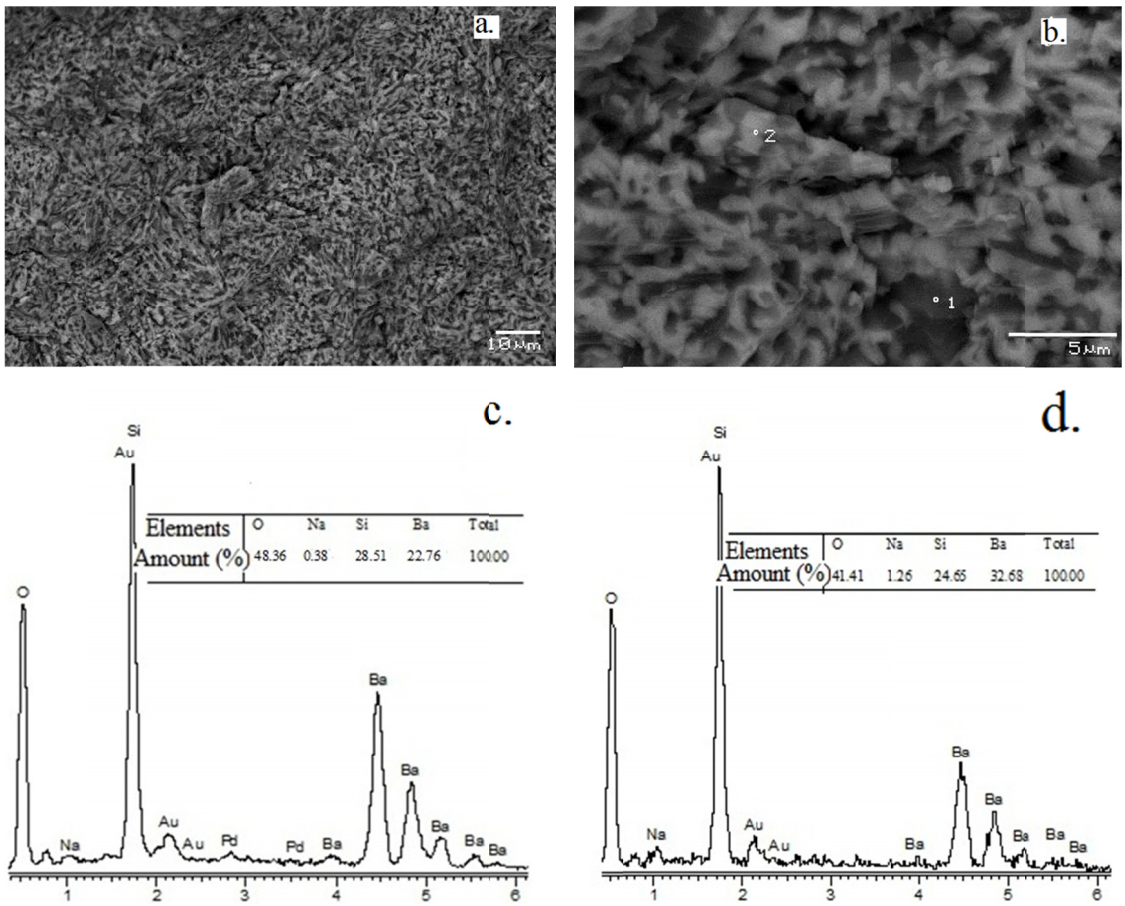

Fig. 5. (a-b) SEM images and (c-d) EDS analysis of the samples heat treated at 800°C

that dark phase is $Li_2O.2SiO_2$ (lithium disilicate) and white one is $BaO.2SiO_2$ (barium disilicate) since Li element is not detectable in the EDS analysis. All EDS analysis showed a high content of Si, indicating SiO_2 as the main ingredient of this glass. After heat treatment at 720°C for 1 h, $Li_2O.2SiO_2$ phase grew to form elongated morphology whereas white $BaO.2SiO_2$ phase formed fibers inside the matrix. Also in Wang et al.'s study the crystallization temperatures as low as 702 and 748°C were applied and long $Li_2O.2SiO_2$ crystals were obtained [10]. In contrast to Höland et al.'s study [11] where no $Li_2O.2SiO_2$ crystals formed in a range of 590-750°C, the present study showed that after 720°C $Li_2O.2SiO_2$ crystals were present. Lithium disilicate crystals had an elongated shape in c-axis with aspect ratios from 2 to 6 in the study of Cramer et al. [12] EDS analysis results corresponding to the samples heat treated at 720°C, confirmed that two distinct phases belong to $Li_2O.2SiO_2$ and $BaO.2SiO_2$ phases. After heat treatment at the highest crystallization temperature,i.e 800°C, the microstructure became finer and a complete mixture of both phases was achieved as shown in Fig. 5. The microstructure after 800°C is similar to that in Apel et al.'s study [13]. In that study, the crystallization temperature was comparable to that in the present study and the microstructure is composed of flakes at very high magnification. These flakes seem finer at low magnification in the present study [13]. Wen et al. applied a crystallization temperature of 800°C and the resultant microstructure at high magnification is similar to that in the present study [14]. Also in Zheng et al.'s study after a crystallization heat treatment at 810°C, fine microstructure was obtained [9]. According to Goharian et al. in the glass matrix P_2O_5 reacts with Li_2O in Li-rich regions and then forms Li_3PO_4 which precipitates in Li_3PO_4 and $Li_2Si_2O_5$ forms consuming Li_2SiO_3 [15].

EDS analysis corresponding to samples heat treated at 800°C, indicated the presence of Ba element, which is similar to each other. The result of EDS analysis confirmed Goharian et al.'s study [15], that the nucleating agent, P_2O_5 used in this study, was completely diffused in the $Li_2O.2SiO_2$ phase as shown in Fig. 5c and Fig. 5d. The crystal morphology of $Li_2O.2SiO_2$ phase observed by several researchers was given in Table 1.

The crystallization temperatures determined previously, were applied to some of the nucleated samples. After exposure at the optimum nucleation parameters (540°C / 1 h), samples were heat treated at 675, 720 and 800°C for a standard duration of 1 h. Between 675 and 720°C, there was no significant increase in the Vickers hardness. However, heat treatment at 800°C for 1 h, resulted in a highest hardness of 1053.8 Hv (10.3 GPa) as in Fig. 6a.

The composition examined in the present study contains 25% of lithium disilicate phase. Thus the mechanical results were compared with lithium disilicate glasses and glass-ceramics given in the literature. According to Tulyaganov et. al, the microhardness results obtained in lithium disilicate were 5.24 and 5.34 GPa [16], which are slightly lower than the average result and half of the highest result of this study. However, after isothermal heat treatments Huang et. al measured 7.83, 7.24 and 6.39 GPa for the hardness of samples with 60.7, 64.9 and 61.7% of crystallinity respectively [17]. In another study, microhardness of lithium disilicate ceramics was found to be 5.8 GPa [18]. Being the highest (1053.8 Hv) when compared with the literature microhardness values, H_v obtained for $0.25Li_2O.2SiO_2$-$0.75BaO.2SiO_2$ glass showed a large scatter.

Indentation load, P was given as 0.5 kg. Fracture toughness of each nucleated and/or crystallized sample was calculated using mean Vickers hardness (average of 15 indentations) for

TABLE 1

Crystal morphology of $Li_2Si_2O_5$ in several literature studies

Reference	Heat Treatment	Grain size	$Li_2Si_2O_5$ Grain morphology
Apel et al. [20]	500°C/10 min+650°C/20 min+850°C/10 min 500°C/10 min+700°C/20 min+850°C/10 min	0.1-1 µm 3 µm	Needle-like and a flake-like morphology longish rather than round
Wen et al. [21]	Nucleation temperatures: 590-605°C Crystallization temperatures: 780-840°C	0.1-0.5 µm	Transformation from rod-shaped to needle-like
Zheng et al. [16]	620°C/3 h+870°C/2 h 610°C/3 h+770°C/2 h 590°C/3 h+760°C/2 h 600°C/3 h+810°C/2 h	2-5 µm in length	Elongated and interlocking crystals
Wang et al. [17]	748°C/1 h + 848°C/1 h 702°C/1 h+830°C/1 h 674°C/1 h+820°C/1 h 636°C/1 h+ 810°C/1 h	The rod-like crystals; 1-3 µm, with P_2O_5 content, grain size 1 µm in length	Following the increase of P_2O_5 content, rod-like crystals forming an interlocking microstructure transformed to spherical shape
Höland et al. [18]	520°C/10 min + 740°C/20 min + 850°C/10 min	2 µm in length	Plate-like lithium disilicate crystals, interlocking microstructure
Goharian et al. [22]	Following 450°C for 1h to relieve internal stress, heat treatments at 610°C and 780°C	N/A	The interlocking and needle-shaped crystals homogeneously embedded in the glass matrix
Present study	540°C/1 h. + 675°C/1 h 540°C/1 h. + 720°C/1 h 540°C/1 h. + 800°C/1 h	Fine microstructure with slight radial morphology- crystals 10 µm in length	Changing from radial symmetry, firstly to elongated morphology then finally to fine microstructure

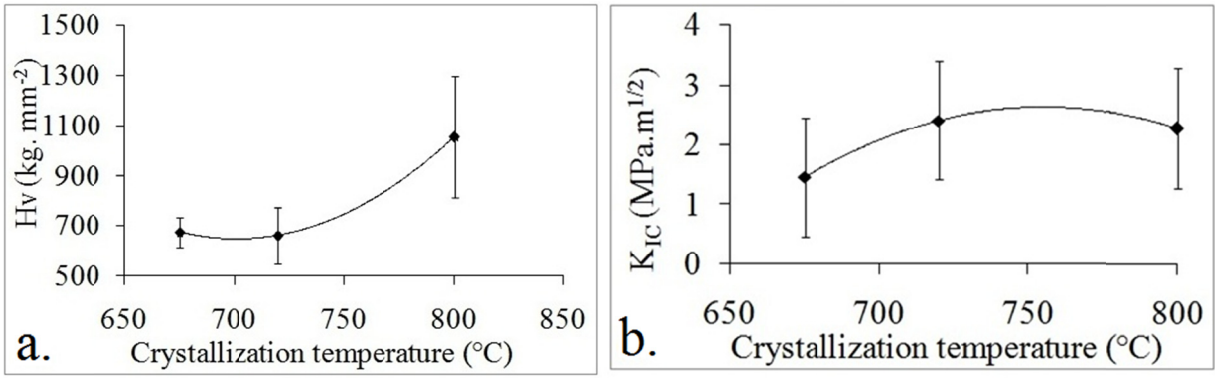

Fig. 6. (a) Vickers indentation data versus crystallization temperature, (b) Indentation fracture toughness versus crystallization temperature

each of them. As an example, for optimum nucleation parameter (540°C / 1h), mean Vickers hardness was measured as 532 Hv (5.2 GPa) and this value was used for the calculation of fracture toughness for this particular sample.

In a study on the lithium disilicate glass-ceramic, K_{IC} values were found to be 2.3 and 2.7 MPa.m$^{1/2}$ [14]. Although the microhardness found in this study is similar to those in the present research, K_{IC} is determined, which is possibly due to low degree of crystallinity of the samples. Since the optimum nucleation temperature was determined to be 540°C, it should be expected that a great amount of crystal nuclei is formed inside the droplets, which in turn increased the indentation fracture toughness. In Fig. 6b, fracture toughness versus crystallization temperatures was given. The highest value was obtained to be 2.4 MPa.m$^{1/2}$ for the sample prepared by two stage heat treatment of 540°C / 1h +720°C / 1h.

Table 2 shows the crack half-length data after indentation under a load of 0.5 kg. The initial crack half-length after the crystallization treatment at 675°C for 1h, was determined to be 35.91 mm. After crystallizing at 800°C, the highest crystallization point, the crack half-length became 23.5 mm.

TABLE 2

Crack half-length data for various crystallization temperatures

Tc (°C)	Crack half length, *c*		
	Mean (mm)	Standard deviation (mm)	Coefficient of variation
675	35.91	5.5	0.63
720	26.24	4.8	0.06
800	23.50	4.8	0.29

The former was sorted from minimum to maximum and for each value, a cumulative probability of occurrence was attributed as P described in Gong and Chen's study [19] by Eq. (1).

$$P = \frac{1-0.5}{15} \tag{1}$$

where $N = 15$ is the number of indentations. P was expressed as a function of K_{IC} as in Eq. (2) as in Fig. 7.

$$\text{Ln Ln}\frac{1}{1-P} = m \text{Ln}\, K_{IC} - m \text{Ln}\, K_0 \tag{2}$$

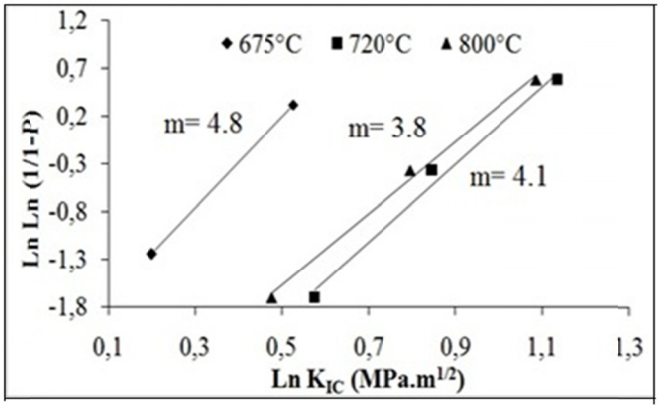

Fig. 7. Weibull plots for indentation fracture toughness data

According to Gong et al.'s study on soda-lime glass, which is also an alkaline-alkaline earth glass, a Weibull modulus of 14.8 was determined [19] which is very consistent with m value for the sample nucleated at 540°C as in Table 3. Kaur et. al has also made studies on lanthanum borosilicate glasses and determined Weibull moduli between 11.93-18.53 [20], which are close to those of the present research for which m values of 5 to 20 are claimed in literature for technical ceramics [5]. Low Weibull modulus exhibits low reliability consequently, fracture toughness is broadly distributed. The scale parameter in this research, K_0 was calculated to be between 0.13-1.02 MPa.m^{½}, which is similar to those in Kaur et al's study [20].

TABLE 3

Weibull parameters for various crystallization temperatures

Tc (°C)	*m*	K_0 (MPa.m$^{1/2}$)
675	4.8	0.46
720	4.1	0.97
800	3.8	0.92

4. Conclusion

The optimum nucleation temperature was determined by DTA analysis to be 540°C. The heat treatment at 540°C led to a maximum decrease in the crystallization temperature, i.e

712°C. SEM results supported with EDS analysis showed that the microstructure consists of two distinct phases, $Li_2O.2SiO_2$ and $BaO.2SiO_2$. Maximum H_v value obtained in this study was 1053.8 Hv (10.3 GPa). The highest value of indentation fracture toughness was obtained to be 2.4 MPa.$m^{1/2}$ for the sample prepared by two stage heat treatment of 540°C / 1h +720°C / 1 h. Weibull modulus, m had a value of approximately 4, which is consistent with literature studies. It was also concluded that as the hardness increased with optimum conditions, the Weibull moduli decreased with a large scatter in fracture toughness as expected.

Acknowledgements

The authors are grateful to Dr. Mustafa İlhan of Marmara University, Department of Metallurgical and Materials Engineering, for performing SEM analysis employed in this study.

REFERENCES

[1] R. Danzer, P. Supancic, J. Pascual, T. Lube, Engineering Fracture Mechanic. **74**, 2919-2932 (2007).
[2] A.D. Bona, K.J. Anusavice, P.H. DeHoff, Dent. Mater. **19**, 662-669 (2003).
[3] A. Saghafi, A.R. Mirhabibi, G.H. Yari, Theoretical and Applied Fracture Mechanics **52**, 180-182 (2009).
[4] G. Lysiak, J. Food Eng. 83, 436-443 (2007).
[5] B. Basu, D. Tiwari, D. Kundu, R. Prasad, Ceram. Int. **35**, 237-246 (2009).
[6] R. Bermejo, P. Supancic, R. Danzer, J. Eur. Ceram. Soc. **32**, 251-255 (2012).
[7] B. Ertug and E. Demirkesen, Trans. Indian Ceram. S. **71**, 95-100 (2011).
[8] A. Marotta, A. Buri, Termochim. Acta. **25**, 155 (1978).
[9] X. Zheng, G. Wen, L. Song, X.X. Huang, Acta Materialia. **56**, 549-558 (2008).
[10] F. Wang, J. Gao, H. Wang, J. Chen, Materials and Design. **31**, 3270-3274 (2010).
[11] W. Höland, E. Apel, Ch van 't Hoen, V. Rheinberger, J. Non-Cryst. Solids. **352**, 4041-4050 (2006).
[12] S. Cramer von Clausbruch, M. Schweiger, W. Höland, V. Rheinberger, J. Non-Cryst. Solids. 263-264, 388-94 (2000).
[13] E. Apel, C van't Hoen, V. Rheinberger, W. Höland, J. Eur. Ceram. Soc. **27**, 1571-1577 (2007).
[14] G. Wen, X. Zheng, L. Song, Acta Mater. **55**, 3583-3591 (2007).
[15] P. Goharian, A. Nemati, M. Shabanian, A. Afshar, J. Non-Cryst. Solids. **356**, 208-214 (2010).
[16] D.U. Tulyaganov, S. Agathopoulos, I. Kansal, P. Valerio, M.J. Ribeiro, J.M.F. Ferreira, Ceram. Int. **35**, 3013-3019 (2009).
[17] S. Huang, P. Cao, C. Wang, Z. Huang, W. Gao, Journal of Asian Ceramic Societies **1**, 46-52 (2013).
[18] H.N. Yoshimura, C.C. Gonzaga, P.F. Cesar, W.G. Miranda Jr., Ceram. Int. **38**, 4715-4722 (2012).
[19] J. Gong, Y. Chen, C. Li, J. Non-Cryst. Solids. **279**, 219-223 (2001).
[20] G. Kaur, O.P. Pandey, K. Singh, J. Non-Cryst. Solids. **358**, 2589-2596 (2012).